Bioconjugate Chemistry

Article

pubs.acs.org/bc

Enhanced Sensitivity Employing Zwitterionic and pI Balancing Dyes (Z-CyDyes) Optimized for 2D-Gel Electrophoresis Based on Side Chain Modifications of CyDye Fluorophores. New Tools For Use in Proteomics and Diagnostics

Mark G. Epstein, Benjamin D. Reeves, Walid S. Maaty, David Fouchard, Edward A. Dratz, Brian Bothner, and Paul A. Grieco*

Department of Chemistry and Biochemistry, Montana State University, PO Box 173400, Bozeman, Montana 59717-3400, United States

Supporting Information

ABSTRACT: The CyDye family of fluorescent dyes is currently the overwhelming choice for applications in proteomic analysis, using two-dimensional difference gel electrophoresis (2D-DIGE). Protein labeling with CyDyes is hampered by protein precipitation and gel smearing when used above minimal labeling. The solubility of labeled protein may be improved by introducing water solubilizing groups on the dye such as cysteic acids. However, addition of a negatively charged functionality will have the undesired effect of shifting the pI in relation to the unlabeled protein. These limitations have been addressed through the synthesis of highly water-soluble and pI balancing zwitterionic CyDye fluorophores (Z-CyDyes). The new dyes feature a cysteic acid motif, a titratable amine functionality and a NHS activated ester group. In side by side 2D-DIGE comparisons of Z-CyDyes and CyDyes, the new dyes significantly enhanced protein spot volume and the number of spots that were detected. Z-CyDyes have the potential to enhance the depth of proteome coverage and provide a general strategy for improving the performance of protein tagging reagents.

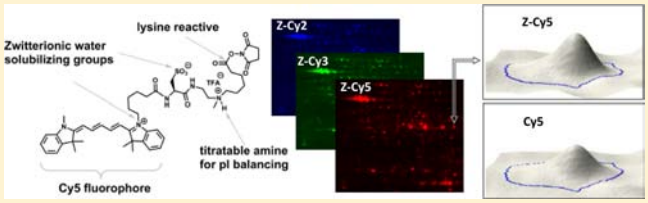

INTRODUCTION

The post-genomic era has sought to provide insight into biological mechanisms, mainly by gaining understanding of the dynamic nature of proteins inferred by their rapid changes in abundance and changes in posttranslational modifications (PTMs) under different biological conditions.[1−3] Most cellular functions are carried out by proteins and are largely regulated by protein PTMs.[4,5] Of the many techniques used to study the proteome, two-dimensional difference gel electrophoresis (2D-DIGE) has long provided insight into the up or down regulation of proteins and protein PTMs, avoiding digestion and uncoupling of PTM combinations before analysis.[6−9] This approach has been applied to the study of many disease states and has led to the identification of potential biomarkers in cancer,[10−14] Alzheimer's Disease,[15−17] and Down's syndrome.[18]

Early seminal work by Minden and co-workers, which led to the synthesis of the commercially available CyDyes and the development of 2D-DIGE,[6] has had some limitations. Structurally CyDyes are nonpolar and decrease the aqueous solubility of labeled proteins,[6,19,20] which may be particularly troublesome when focused at the isoelectric point in the first separation dimension, because this is the pH of minimum solubility of each protein. Since the standard 2D-DIGE method targets dyes to highly abundant lysine residues, protein precipitation with CyDyes will often occur at high levels of labeling.[6] To overcome this problem, minimal labeling protocols are utilized where approximately one percent of the lysine residues present in a protein are labeled, providing fluorescent signals adequate for detection, while minimizing precipitation of the tagged proteins.[6,7]

Alternative approaches to improve sensitivity and 2D-DIGE performance by increasing the dye to protein ratio have been developed in which cysteine residues are selectively targeted.[19,20] However, to improve sensitivity, a large dye to protein ratio must be employed, commonly referred to as saturation labeling. This leads to precipitation of a great many proteins unless very small amounts of protein (a few micrograms) are run on the 2D gels, which limits the ability to identify proteins by mass spectrometry.[19] A further limitation for the use of thiols to measure total protein abundance is their tendency to undergo oxidation to sulfenic acids, sulfinic acids, disulfides, and *S*-nitrosothiols due to oxidative stress, infection, and toxins.[21−23]

There has been intense interest in the derivatization of cyanine dyes with sulfo and sulfoalkyl water solubilizing groups.[24−31] Sulfo groups have been shown to decrease dye aggregation leading to better water solubility and photostability.[32,33] While the spectroscopic properties of these dyes have been thoroughly studied, the charged solubilizing groups lead to substantial pI shift due to protein labeling when employed in

Received: March 28, 2013
Revised: July 24, 2013
Published: July 24, 2013

2D-DIGE experiments, which hampers automated spot picking. There remains the need for more water-soluble dyes designed specifically for 2D-DIGE minimal labeling with pI balancing capability.

Herein we describe the synthesis of highly water-soluble and pI balancing zwitterionic CyDyes (Z-CyDyes), which possess the following features: (1) a CyDye fluorophore, (2) a cysteic acid group, (3) a titratable amine, and (4) an amine reactive succinimidyl ester (Figure 1). The cysteic acid imparts water

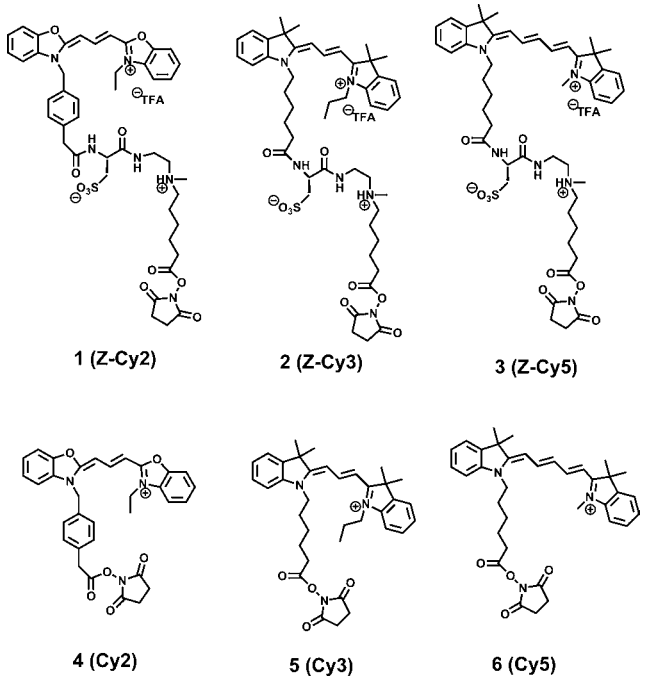

Figure 1. Structure of Z-CyDyes **1**−**3** and CyDye DIGE fluors Cy2 (**4**), Cy3 (**5**), and Cy5 (**6**).

solubility, while the titratable amine balances protein pI by partially compensating for the loss of a lysine side chain upon labeling. In addition we demonstrate that Z-CyDyes **1**−**3** provide significantly enhanced detection sensitivity relative to the DIGE fluor minimal CyDyes (cf. **4**−**6**, Figure 1).

SYNTHESIS PROCEDURES

General. Nuclear magnetic resonance, both proton (^{1}H NMR) and carbon (^{13}C NMR), were recorded using either a 300 MHz Bruker Avance DPX 300 spectrometer or a 500 MHz Bruker Avance DRX 500 spectrometer, and all reports are given in parts per million (δ). FTIR spectra was acquired on a JASCO FT/IR 4100 or a Perkin-Elmer 1600 series. Reactions were monitored using reverse phase HPLC utilizing a Shimadzu CBM-2A Prominence Communications Bus Module, Shimadzu SPD-M20A Prominence Diode Array Detector, LC-20AB Prominence Liquid Chromatograph, and a Phenomenex Synergi 4 μ Polar RP 80 Å 250 × 10.00 mm column. The mobile phase was always a gradient of HPLC grade H_2O: 95% CH_3CN, 5% H_2O containing 0.1% HPLC grade TFA. Reverse phase HPLC purification was carried out using a Waters 600 Pump, a Waters 600 Controller, and a Waters 2487 Dual λ Absorbance Detector utilizing a preparative reverse phase Phenomenex Synergi 4 μ Polar RP 80 Å AXIF 250 mm × 21.20 mm column. High resolution mass spectrometry analyses were performed by the University of Notre Dame Mass Spectrometry Laboratory. Unless noted otherwise all reactions were run under argon using anhydrous solvents. All anhydrous solvents were obtained from SIGMA-Aldrich in Sure/Seal bottles. All other reagents were obtained from SIGMA-Aldrich and used as received. Triethylamine and *N*-methylmorpholine were distilled over CaH_2. Pyridine was distilled over CaO. Cy2, Cy3,and Cy5 were synthesized following the protocol of Jung.[34]

Synthesis: *tert*-Butyl 6-(2,2,2-trifluoro-*N*-methylacetamido)hexanoate (7). *N*-Methylcaprolactam (12.9 g, 13 mL, 101 mmol) was dissolved in 6 M HCl (100 mL) and the solution was heated to reflux overnight. The solvent was removed *in vacuo* to yield an orange liquid which was treated with benzene (250 mL) and refluxed through a Dean−Stark trap for 5 h. The solvent was removed *in vacuo* to give 32.66 g of crude 6-(methylamino)hexanoic acid hydrochloric acid: ^{1}H NMR (D_2O, 300 MHz): δ 1.25 (m, 2H), 1.43−1.59 (m, 4H), 2.24 (t, 2H, J = 7.2 Hz), 2.54 (s, 3H), 2.87 (t, 2H, J = 7.5 Hz).

The resulting solid (3.62 g, 19.9 mmol) was dissolved in anhydrous methanol (10 mL) at 0 °C under argon followed by triethylamine (8.30 mL, 59.7 mmol) addition. After stirring the resulting mixture at 0 °C for 5 min, trifluoromethyl acetate (2.39 mL, 23.9 mmol) was added dropwise and the resulting mixture was stirred at ambient temperature for 16 h. The solvent was removed *in vacuo* and the resulting solid was dissolved in H_2O, acidified to pH 3 using 1 M HCl, and extracted with ethyl acetate (4 × 10 mL). The organic layer was washed with water (2 × 10 mL) and brine (10 mL) and was dried over sodium sulfate. The solvent was removed *in vacuo* to provide 6-(2,2,2-trifluoro-*N*-methylacetamido)hexanoic acid as a light brown oil (4.65 g, 19.3 mmol, 97%): FTIR (cm^{-1}): 3105, 3034, 2946, 2870, 1691, 1462, 1415, 1247, 1189, 1144, 1105, 1082, 926, 758; ^{1}H NMR ($CDCl_3$, 500 MHz): δ 1.20−1.26 (m, 2H), 1.46−1.57 (m, 4H), 2.23 and 2.24 (2t, J = 7.5 Hz, total of 2H), 2.99 and 2.89 (2s, total of 3H), 3.31 and 3.27 (2t, J = 7.5 Hz, total of 2H); ^{13}C NMR ($CDCl_3$, 125 MHz): δ [24.02, 24.07], 25.63, [25.76, 25.91], 27.73, 33.61, [34.20, 34.60], [49.05, 49.24], 116.45 (qd, J = 285 Hz, J = 8 Hz), 156.68 (q, J = 35 Hz), [179.32, 179.13]; HRMS-ESI (m/z): $[M+H]^+$ calcd for $C_9H_{14}F_3NO_3^+$ 242.0999, Found 242.0976.

Distilled pyridine (656 μL, 8.12 mmol) was added to a solution of 6-(2,2,2-trifluoro-*N*-methylacetamido)hexanoic acid (982 mg, 4.06 mmol) in anhydrous dichloromethane (20 mL) at rt. *tert*-Butanol (2.33 mL, 48.0 mmol) and $POCl_3$ (752 μL, 8.12 mmol) were added dropwise and the mixture was stirred at rt for 21 h. DCM (20 mL) was added and the organic layer was washed with H_2O (3×) and brine (2×). The solvent was dried with sodium sulfate and removed *in vacuo*. The product was purified using DAVISIL (dichloromethane) to provide **7** as a clear oil (724 mg, 2.44 mmol, 60%): FTIR (cm^{-1}): 2979, 2939, 2868, 1729, 1697, 1459, 1421, 1392, 1368, 1308, 1144, 1103, 1082, 757; ^{1}H NMR ($CDCl_3$, 500 MHz): δ 1.13−1.24 (m, 2H), 1.32 (s, 9H), 1.44−1.55 (m, 4H), 2.08−2.12 (m, 2H), 2.89 and 2.99 (2s, total of 3H), 3.27 and 3.31 (2t, J = 7.5 Hz, total of 2H); ^{13}C NMR ($CDCl_3$, 125 MHz): δ [24.55, 24.45], [25.88, 25.69], 26.05, [27.91, 27.85], [34.58, 34.16], [35.12, 35.04], [49.27, 49.10], [80.03, 79.93], 116.46 (qd, J = 285 Hz, J = 7.5 Hz), [156.74, 156.45], [172.72, 172.60]; HRMS-ESI (m/z): $[M+H]^+$ calcd for $C_{13}H_{23}F_3NO_3^+$ 298.1625, Found 298.1610.

Sodium 6-(*N*-methyl-*N*-(2-(2-*tert*-butoxycarbonylamino-3-tritylsulfanyl-propionamido)ethyl)amino)-hexanoate (8). A solution of LiOH (47 mg, 1.96 mmol) in H_2O (2 mL) was added slowly to a stirred solution of **7** (530 mg,

dx.doi.org/10.1021/bc4002213 | *Bioconjugate Chem.* 2013, 24, 1552−1561

1.78 mmol) in MeOH (4 mL) at 0 °C. The mixture was stirred at 0 °C for 5 min, followed by stirring at ambient temperature for 4 h. The methanol was removed *in vacuo*, and water (92 mL) was added. The product was isolated by extraction with ethyl acetate. The organic extract was dried with sodium sulfate and removed *in vacuo*. The residue was purified by flash chromatography on triethylamine deactivated DAVISIL (9:1 dichloromethane:methanol) providing *tert*-butyl-6-(methylamino)-hexanoate as a yellow oil (344 mg, 1.71 mmol, 96%): ^{1}H NMR (500 MHz, $CDCl_3$): δ 1.35−1.42 (m, 2H), 1.41 (s, 9H), 1.59 (p, J = 7.5 Hz, 2H), 1.85 (p, J = 7.5 Hz, 2h), 2.20 (t, J = 7.5 Hz, 2H), 2.65 (s, 3H), 2.91 (t, J = 7.5 Hz, 2H); ^{13}C NMR ($CDCl_3$, 125 MHz): δ 24.51, 25.75, 26.25, 28.27, 33.01, 35.28, 49.34, 80.39, 172.81; HRMS-ESI (m/z): $[M+H]^+$ calcd for $C_{11}H_{24}NO_2^+$ 202.1807, Found 202.1804.

tert-Butyl-6-(methylamino)hexanoate (205 mg, 1.02 mmol), *tert*-butyl 2-bromoethylcarbamate (202 mg, 0.903 mmol), and Na_2CO_3 (316 mg, 2.97 mmol) were treated with a mixture of H_2O (1.8 mL) and 1,4-dioxane (1.8 mL). The mixture was stirred at 80 °C for 3 h and allowed to cool to room temperature and the solvents were removed *in vacuo*. The resulting solid was partitioned between H_2O and DCM, and the aqueous phase was extracted with DCM (3×). The combined organic extracts were dried over $MgSO_4$ and the solvent was removed *in vacuo* to yield crude *tert*-butyl-2-(*N*-methyl-*N*-(5-(*tert*-butoxycarbonyl) hexylamino))ethylcarbamate which was used in the next step without further purification (270 mg, 0.785 mmol).

Triethylsilane (1.44 mL, 9.04 mmol) was added to a solution of *tert*-butyl-2-(*N*-methyl-*N*-(5-(*tert*-butoxycarbonyl)hexylamino))-ethylcarbamate (1.44 g, 4.19 mmol) in TFA (10 mL) and DCM (10 mL) and the mixture was stirred at rt for 1 h. Solvents were removed *in vacuo* and the residue partitioned between H_2O and Et_2O. The aqueous phase was evaporated *in vacuo* to yield crude 6-(*N*-(2-aminoethyl)-*N*-methylamino)-hexanoic acid trifluoroacetate which was used in the next step without further purification.

A solution of 6-(*N*-(2-aminoethyl)-*N*-methylamino)hexanoic acid trifluoroacetate (4.19 mmol), Boc-Cys(Trt)-OSu (4.69 g, 8.37 mmol), and Na_2CO_3 (1.77 g, 16.7 mmol) in H_2O (40 mL) and 1,4-dioxane (40 mL) was stirred at rt for 48 h. The 1,4-dioxane was removed *in vacuo* and the resulting solution was extracted with EtOAc. The EtOAc extract was dried over Na_2SO_4 and the solvent was removed *in vacuo*. The residue was purified by flash chromatography on DAVISIL (10 to 20% MeOH in DCM) to yield a white solid (2 g, 3.07 mmol, 56% over 3 steps): FTIR (cm^{-1}): 3405, 3320, 3057, 2977, 2931, 1711, 1490, 1366, 1167, 741, 701; ^{1}H NMR (500 MHz, CD_3OD): δ 1.36 (p, 2H, J = 7.5 Hz), 1.44 (s, 9 H), 1.62 (p, 2H, J = 7.5 Hz), 2.21 (t, 2H, J = 7.5 Hz), 2.45−2.57 (m, 2H), 2.64 (s, 3H), 2.87 (t, 2H, J = 7.5 Hz), 2.96 (br, 2H), 337−3.51 (m, 2H), 3.92 (t, 1H, J = 6.5 Hz), 7.23 (t, 3H, J = 7.5 Hz), 7.29 (t, 6H, J = 7.5 Hz), 7.37 (d, 6H, J = 7.5 Hz); ^{13}C NMR (125 MHz, CD_3OD): δ 26.06, 26.45, 27.69, 28.86, 35.30, 36.77, 37.35, 41.66, 55.49, 56.87, 58.16, 68.20, 81.16, 128.11, 129.17, 130.87, 146.11, 157.58, 173.85, 180.79; HRMS-ESI (m/z): $[M+H]^+$ calcd for $C_{36}H_{45}N_3O_5S^+$ 634.3314, Found 634.3312.

6-(*N*-Methyl-*N*-(2-(2-amino-3-sulfatopropionamido)-ethyl)amino)hexanoic Acid (9). Triethylsilane (0.036 mL, 0.222 mmol) was added to a solution of **8** (72 mg, 0.111 mmol) in TFA (1 mL) and DCM (1 mL) and the mixture was stirred at room temperature under argon for 1 h. Solvents were removed *in vacuo* and the residue partitioned between H_2O and Et_2O. The aqueous phase was evaporated *in vacuo* to yield 6-(*N*-methyl-*N*-(2-(2-amino-3-thiopropionamido)ethyl)-amino)hexanoic acid as a white solid. A performic acid reagent solution (a mixture of 30% hydrogen peroxide (5 mL) and 99% formic acid (50 mL) that was allowed to stand at rt for 1 h prior to use, 18 mL) was added to 6-(*N*-methyl-*N*-(2-(2-amino-3-thiopropionamido)ethyl)amino)hexanoic acid at 0 °C and the solution was stirred for 1 h. The solvent was removed *in vacuo*. Water was added and removed *in vacuo* again to yield **9** as a white solid (0.038 mg, 0.111 mmol, 100%): FTIR (cm^{-1}): 3423, 3087, 2956, 2876, 1684, 1202, 1134, 1042, 721; ^{1}H NMR (500 MHz, D_2O): δ 1.19 (bs, 2H), 1.42−1.45 (m, 2H), 1.55−1.69 (m, 2H), 2.20−2.22 (m, 2H), 2.70 (d, 3H, J = 4.5 Hz), 3.07−3.18 (m, 1H), 3.21−3.34 (m, 2H), 3.22−3.47 (m, 4H), 3.63−3.68 (m, 1H), 4.22 (bs, 1H); ^{13}C NMR (125 MHz, D_2O): δ 23.00, 23.59, 25.01, 33.36, [34.50, 34.57], 39.85, [49.84, 50.01], [54.58, 54.65], [56.17, 56.49], 168.26, 178.59; HRMS-ESI (m/z): $[M]^+$ calcd for $C_{12}H_{26}N_3O_6S^+$ 340.1542, found 340.1514.

(2*R*)-3-((2-((5-Carboxypentyl)(methyl)ammonio)-ethyl)amino)-2-(2-(4-((2-((1*E*,3*Z*)-3-(3-ethylbenzo[*d*]-oxazol-2(3*H*)-ylidene)prop-1-en-1-yl)benzo[*d*]oxazol-3-ium-3-yl)methyl)phenyl)acetamido)-3-oxopropane-1-sulfonate 2,2,2-trifluoroacetate (10). 2-[3-[3-[[4-[2-[(2,5-Dioxo-1-pyrrolidinyl)oxy]-2-oxoethyl]phenyl]methyl]-2(3*H*)-benzo-xazolylidene]-1-propenyl]-3-ethyl-benzoxazolium salt **4** (46.9 mg, 0.071 mmol, 1.0 equiv) was stirred in dimethylformamide (5.0 mL) with **9** (160.1 mg, 0.35 mmol, 5.0 equiv) at rt. To the stirring solution was added 4-methylmorpholine (0.15 mL, 1.4 mmol, 20.0 equiv) in a dropwise fashion. The reaction mixture was stirred for 24 h, after which the solvent was removed under lyophilization yielding crude product as a deep yellow oil. Purification was performed via reverse phase HPLC (30 to 70% B, 20 mL/min, 30 min, 450 nm, Rt = 15−18 min) providing 29.0 mg (46% yield) of the TFA salt (**10**) as a deep yellow powder: FTIR (cm^{-1}): 3357, 2922, 2851, 1681, 1565, 1509; ^{1}H NMR (300 MHz, CD_3OD): δ 1.25−1.39 (m, 2H), 1.46 (t, J = 7.5 Hz, 3H), 1.59−1.82 (m, 2H), 2.30 (t, 2H, J = 7.2 Hz), 2.85 (s, 3H), 3.09−3.25 (m, 4H), 3.45−3.59 (m, 6H), 4.25 (q, J = 7.5 Hz, 2H), 4.62 (dd, J = 7.5, 3.9 Hz, 1H), 5.42 (s, 2H), 6.01 (d, J = 13.2 Hz, 1H), 6.04 (d, J = 13.5 Hz, 1H), 7.32−7.63 (m, 12H), 8.60 (dd, J = 13.5, 13.2 Hz, 1H); ^{13}C NMR (125 MHz, CD_3OD): δ 13.37, 24.76, 25.54, 27.15, 34.66, 35.43, 40.59, 43.28, 52.30, 57.31, 57.35, 57.68, 86.01, 87.07, 112.01, 112.04, 112.13, 112.25, 112.39,112.43, 126.51, 126.58, 126.83, 127.41, 127.53, 128.76, 131.42, 132.37, 132.90, 132.99, 134.02, 137.15, 139.86, 148.53, 148.68, 149.37, 163.82, 164.26, 173.57; HRMS-ESI (m/z): Exact mass calcd for $C_{40}H_{48}N_5O_9S$ $[M]^+$ 774.3167, found 774.3168.

(2*R*)-3-((2-((6-((2,5-Dioxopyrrolidin-1-yl)oxy)-6-oxo-hexyl) (methyl)ammonio)ethyl)amino)-2-(2-(4-((2-((1*E*,3*Z*)-3-(3-ethylbenzo[*d*]oxazol-2(3*H*)-ylidene)prop-1-en-1-yl)benzo[*d*]oxazol-3-ium-3-yl)methyl)phenyl)-acetamido)-3-oxopropane-1-sulfonate 2,2,2-trifluoroacetate (1). Compound **10** (4.9 mg, 0.006 mmol, 1.0 equiv) was stirred in dimethylformamide (0.5 mL) with *N*-hydroxy-succimide (7.0 mg, 0.061 mmol, 11 equiv) at rt. To the stirring solution was added *N,N′*-diisopropylcarbodiimide (8.0 μL, 0.050 mmol, 9.0 equiv) in a dropwise fashion. The reaction mixture was stirred for 18 h, after which the solvent was removed under lyophilization yielding crude product as a deep yellow oil. Purification was performed via reverse phase HPLC (30 to 70% B, 20 mL/min, 30 min, 450 nm, Rt = 19−21 min) providing 4.0 mg (82% yield) of the TFA salt (**1**) as a deep

yellow powder: FTIR (cm^{-1}): 3331, 3063, 2938, 2858, 1741, 16712, 1560, 1507, 1461; ^1H NMR (300 MHz, CD_3OD): δ 1.23−1.41 (m, 2H), 1.45 (t, J = 7.5 Hz, 3H), 1.69−1.85 (m, 4H), 2.66 (t, J = 7.2 Hz, 2H), 2.81 (s, 4H), 2.85 (s, 3H), 3.10−3.25 (m, 4H), 3.46−3.66 (m, 6H), 4.25 (q, J = 7.5 Hz, 2H), 4.58−4.66 (m, 1H), 5.41 (s, 2H), 6.00 (d, J = 13.2 Hz, 1H), 6.05 (d, J = 13.2 Hz, 1H), 7.34−7.66 (m, 12H), 8.29−8.44 (m, 1H) (NH), 8.59 (t, J = 13.2 Hz, 1H); ^{13}C NMR (125 MHz, CD_3OD): δ 13.39, 24.50, 25.16, 25.19, 26.22, 26.65, 31.39, 34.92, 35.36, 35.42, 40.60, 40.90, 40.97, 43.26, 43.31, 52.32, 53.00, 53.15, 57.37, 57.55, 86.00, 87.07, 112.01, 112.13, 112.25, 112.38, 126.57, 126.83, 127.41, 127.53, 128.78, 131.42, 131.45, 132.36, 132.99, 134.02, 137.12, 137.18, 148.52, 148.67, 149.25, 149.33, 163.80, 164.24, 170.31, 172.02, 173.49, 173.56; HRMS-ESI (m/z): Exact mass calcd for $C_{44}H_{51}N_6O_{11}S$ $[M]^+$ 871.3331, found 871.3336.

(2*R*)-3-((2-((5-Carboxypentyl)(methyl)ammonio)-ethyl)amino)-2-(6-(2-((*E*)-3-((*E*)-3,3-dimethyl-1-propylindolin-2-ylidene)prop-1-en-1-yl)-3,3-dimethyl-3*H*-indol-1-ium-1-yl)hexanamido)-3-oxopropane-1-sulfonate 2,2,2-trifluoroacetate (11). 2-[3-(1,3-Dihydro-3,3-dimethyl-1-propyl-2*H*-indol-2-ylidene)-1-propenyl]-1-[6-[(2,5-dioxo-1-pyrro-lidinyl)oxy]-6-oxohexyl]-3,3-dimethyl-3*H*-indolium salt **5** (15.5 mg, 0.022 mmol, 1.0 equiv) was stirred in dimethylformamide (1.6 mL) with **9** (50.33 mg, 0.11 mmol, 5.0 equiv) at rt. To the stirring solution was added 4-methylmorpholine (0.048 mL, 0.44 mmol, 20.0 equiv) in a dropwise fashion. The reaction mixture was stirred for 20 h, after which the solvent was removed under lyophilization yielding crude product as a deep red oil. Purification which was performed via reverse phase HPLC (40 to 80% B, 20 mL/min, 30 min, 530 nm, Rt = 12−16 min) provided 15.9 mg (79% yield) of the TFA salt (**11**) as a deep red powder: FTIR (cm^{-1}): 3624, 2938, 1681, 1558, 1478. ^1H NMR (300 MHz, CD_3OD): δ 1.08 (t, 3H, J = 7.3 Hz), 1.28−1.92 (m, 26H), 2.29−2.34 (m, 4H), 2.87 (s, 3H), 2.98−3.24 (m, 4H), 3.44−3.72 (m, 4H), 4.10−4.20 (m, 4H), 4.65−4.69 (m, 1H), 6.49 (d, J = 13.2 Hz, 1H), 6.52 (d, J = 13.2 Hz, 1H), 7.28−7.56 (m, 8H), 8.40−8.47 (m, 1H) (NH), 8.56 (t, J = 13.2 Hz, 1H); ^{13}C NMR (125 MHz,CD_3OD): δ 11.64, 22.07, 24.79, 25.55, 26.30, 27.16, 27.31, 28.33, 28.48, 34.66, 35.37, 35.45, 36.67, 40.86, 40.94, 45.23, 46.79, 50.78, 50.83, 52.02, 52.06, 53.16, 53.26, 57.28, 57.35, 57.68, 103.74, 104.00, 112.66, 112.71, 123.67, 126.91, 130.14, 130.21, 142.33, 142.39, 143.54, 143.64, 152.35, 173.70, 175.61, 175.64, 176.09, 176.36, 177.30, 177.34; HRMS-ESI (m/z): Exact mass calcd for $C_{44}H_{64}N_5O_7S$ $[M]^+$ 806.4521, found 806.4538.

(2*R*)-2-(6-(2-((*E*)-3-((*E*)-3,3-Dimethyl-1-propylindolin-2-ylidene)prop-1-en-1-yl)-3,3-dimethyl-3*H*-indol-1-ium-1-yl)hexanamido)-3-((2-((6-((2,5-dioxopyrrolidin-1-yl)oxy)-6 oxohexyl)(methyl)ammonio)ethyl)amino)-3-oxopropane-1-sulfonate 2,2,2-trifluoroacetate (2). Compound **11** (6.3 mg, 0.0068 mmol, 1.0 equiv) was stirred in dimethylformamide (0.6 mL) with *N*-hydroxysuccimide (8.6 mg, 0.075 mmol, 11 equiv) at rt. To the stirring solution was added *N,N′*-diisopropylcarbodiimide (9.5 μL, 0.061 mmol, 9.0 equiv) in a dropwise fashion. The reaction mixture was stirred for 22 h, after which the solvent was removed under lyophilization yielding crude product as a deep red oil. Purification was performed via reverse phase HPLC (40 to 70% B, 20 mL/min, 40 min, 530 nm, Rt = 15−17 min) providing 3.3 mg (48% yield) of the TFA salt (**2**) as a deep red powder: FTIR (cm^{-1}): 3316, 2968, 2935, 2870, 1745, 1560, 1457, 1430; ^1H NMR (300 MHz, CD_3OD): δ 1.08 (t, J = 7.3, 2H), 1.44−2.03 (m, 26H), 2.28−2.32 (m, 2H), 2.66 (q, J = 6.9 Hz, 2H), 2.81 (s, 2H), 2.83 (s, 2H), 2.95 (s, 3H), 3.00−3.25 (m, 4H), 3.38−3.77 (m, 4H), 4.13−4.17 (m, 4H), 4.67 (dd, J = 7.5, 5.1, 1H), 6.49 (d, J = 13.2 Hz, 1H), 6.52 (d, J = 13.2 Hz, 1H), 7.28−7.56 (m, 8H), 8.40−8.46 (m, 1H) (NH), 8.55 (t, J = 13.5 Hz, 1H); ^{13}C NMR (125 MHz, CD_3OD): δ 11.64, 22.06, 24.53, 25.17, 25.20, 26.29, 26.65, 26.70, 27.31, 28.33, 28.49, 31.40, 35.39, 35.45, 36.66, 36.68, 40.93, 41.00, 45.24, 46.80, 50.73, 50.77, 50.82, 52.04, 52.08, 53.16, 53.26, 57.31, 57.34, 57.57, 103.76, 104.01, 112.66, 112.70, 123.67, 126.89, 126.90, 130.12, 130.20, 142.33, 142.38, 143.53, 143.64, 152.33, 170.30, 171.99, 172.00, 173.69, 175.62, 175.64, 176.08, 176.35; HRMS-ESI (m/z): Exact mass calcd for $C_{48}H_{67}N_6O_9S$ $[M]^+$ 903.4685, found 903.4701.

(2*R*)-3-((2-((5-Carboxypentyl)(methyl)ammonio)-ethyl)amino)-2-(6-(3,3-dimethyl-2-((1*E*,3*E*)-5-((*E*)-1,3,3-trimethylindolin-2-ylidene)penta-1,3-dien-1-yl)-3*H*-indol-1-ium-1-yl)hexanamido)-3-oxopropane-1-sulfonate 2,2,2-trifluoroacetate (12). 2-[5-(1,3-Dihydro-1,3,3-trimethyl-2*H*-indol-2-ylidene)-1,3-pentadienyl]-1-[6-[(2,5-dioxo-1-pyrrolidi-nyl)oxy]-6-oxohexyl]-3,3-dimethyl-3*H*-indolium salt, **6** (22.8 mg, 0.032 mmol, 1.0 equiv) was stirred in dimethylformamide (2.2 mL) with **9** (74.4 mg, 0.16 mmol, 5.0 equiv) at rt. To the stirring solution was added 4-methylmorpholine (0.07 mL, 0.64 mmol, 20.0 equiv) in a dropwise fashion. The reaction mixture was stirred for 25 h, after which the solvent was removed under lyophilization yielding the crude product as a deep blue oil. Purification which was performed via reverse phase HPLC (60 to 90% B, 20 mL/min, 30 min, 600 nm, Rt = 12−15 min) afforded 22.5 mg (77% yield) of the TFA salt **12** as a deep blue powder: FTIR (cm^{-1}): 3545, 2963, 2865, 1682, 1653, 1540, 1496, 1482, 1455; ^1H NMR (300 MHz, CD_3OD): δ 1.3−1.69 (m, 6H), 1.73 (s,12), 1.78−1.88 (m, 4H), 2.26−2.36 (m, 4H), 2.88 (s, 3H), 3.00−3.26 (m, 4H), 3.44−3.60 (m, 2H), 3.64 (s, 3H), 3.69−3.87 (m, 2H), 4.10 (t, J = 7.2 Hz, 2H), 4.65−4.69 (m, 1H), 6.34 (d, J = 13.8, 1H), 6.36 (d, J = 13.8, 1H), 6.68 (t, J = 12.3,1H), 7.24−7.51 (m, 8H), 8.25 (dd, J = 13.8, 12.3 Hz, 2H), 8.43−8.46 (m, 1H) (NH); ^{13}C NMR (125 MHz, CD_3OD): δ 24.78, 24.82, 25.56, 26.25, 27.19, 27.96, 28.11, 28.22, 31.77, 34.66, 35.35, 35.45, 36.44, 40.90, 44.94, 50.66, 52.09, 53.26, 53.33, 57.28, 57.35, 57.63, 57.74, 104.46, 104.77, 112.01, 112.19, 123.42, 123.56, 126.35, 126.41, 126.84, 129.87, 129.95, 142.72, 142.79, 143.71, 144.43, 155.65, 155.77, 173.74, 174.75, 175.61, 175.65; HRMS-ESI (m/z): Exact mass calcd for $C_{44}H_{62}N_5O_7S$ $[M]^+$ 804.4364, found 804.4352.

(2*R*)-2-(6-(3,3-Dimethyl-2-((1*E*,3*E*)-5-((*E*)-1,3,3-trimethylindolin-2-ylidene)penta-1,3-dien-1-yl)-3*H*-indol-1-ium-1-yl)hexanamido)-3-((2-((6-((2,5-dioxopyrrolidin-1-yl)oxy)-6-oxohexyl)(methyl)ammonio)ethyl)amino)-3-oxopropane-1-sulfonate 2,2,2-trifluoroacetate (3). Compound **12** (20.6 mg, 0.022 mmol, 1.0 equiv) was stirred in dimethylformamide (2.0 mL) with *N*-hydroxysuccimide (28.3 mg, 0.25 mmol, 11.0 equiv) at rt. To the stirring solution was added *N,N′*-diisopropylcarbodiimide (31 μL, 0.19 mmol, 9.0 equiv) in a dropwise fashion. The reaction mixture was stirred for 20 h, after which the solvent was removed under lyophilization yielding the crude product as a deep blue oil. Purification was performed via reverse phase HPLC (60 to 90% B, 20 mL/min, 30 min, 600 nm, Rt = 15−18 min) providing 17.0 mg (76% yield) of the TFA salt (**3**) as a deep blue powder: FTIR (cm^{-1}) 3339, 2941, 2866, 1741, 1672, 1495, 1457; ^1H NMR (300 MHz, CD_3OD): δ 1.47−1.56 (m, 4H), 1.73 (s, 12H), 1.77−1.83

dx.doi.org/10.1021/bc4002213 | *Bioconjugate Chem.* 2013, 24, 1552−1561

(m,8H), 2.26−2.31 (m, 2H), 2.62−2.70 (m, 2H), 2.80 (s, 2H), 2.82 (s, 2H) 2.89 (s, 3H), 3.00−3.27 (m, 6H), 3.37−3.48 (m, 2H), 3.64 (s, 3H), 4.10 (t, 2H, J = 7.2 Hz), 4.65−4.69 (m, 1H), 6.33−6.41 (m, 2H), 6.65−6.74 (m, 1H), 7.23−7.50 (m, 8H), 8.25 (dd, J = 13.3, 13.2 Hz, 2H), 8.41−8.47 (m, 1H) (NH); ^{13}C NMR (125 MHz, CD_3OD): δ 24.52, 24.58, 25.16, 25.23, 26.25, 26.64, 26.74, 27.13, 27.17, 27.96, 28.12, 31.41, 31.78, 35.35, 35.43, 36.41, 40.93, 41.00, 44.97, 50.65, 52.12, 53.26, 53.34, 57.32, 57.35, 57.45, 57.63, 104.47, 104.81, 112.00, 112.17,123.43, 123.56, 126.34, 126.40, 126.86, 129.86, 129.94, 142.73, 142.79, 143.70,144.44, 155.64, 155.77, 170.27, 170.31, 171.98, 172.00, 173.74, 174.73, 175.59, 175.62; HRMS −ESI (m/z): Exact mass calcd for $C_{48}H_{65}N_6O_9S$ $[M]^+$ 901.4528, found 901.4553.

1-Ethyl-2-((1*E*,3*E*)-5-((*E*)-1-ethyl-3,3-dimethylindolin-2-ylidene)penta-1,3-dien-1-yl)-3,3-dimethyl-3*H*-indol-1-ium 2,2,2-trifluoroacetate (13). To a round-bottom flask charged with absolute ethanol (135 mL) and equipped with a stir bar was added 1-ethyl-2,3,3-trimethyl-3*H*-indolium bromide (460.0 mg, 1.7 mmol, 1.0 equiv) and 2-(4-phenylamino-1*E*,3*E*-butadien-1-yl)-1-ethyl-3,3-dimethylindolium chloride (605.0 mg, 1.7 mmol, 1.0 equiv) followed by sodium acetate (168 mg, 2.1 mmol, 1.2 equiv) and the reaction mixture was refluxed for 3.5 h. The solvent was removed via rotary evaporation followed by drying under lyophilization yielding the crude product as a deep blue oil. Purification was performed via reverse phase HPLC (40 to 70% B, 20 mL/min, 40 min, 600 nm, Rt = 29−36 min) providing 63.3 mg (5% yield) of TFA salt (**13**) as a deep blue powder: FTIR (cm^{-1}) 2969, 2878, 1723, 1684, 1570, 1486, 1453. ^{1}H NMR (500 MHz, CD_3OD): δ 1.38 (t, J = 7.5, 6H), 1.71 (s, 12H), 4.14 (q, J = 7.5, 4H), 6.27 (d, 2H, J = 13.5), 6.62 (t, J = 12.5, 1H), 7.24−7.39 (m, 4H), 7.41−7.42 (m, 2H), 7.48−7.49 (m, 2H), 8.24 (dd, J = 13.5, 12.5, 2H); ^{13}C NMR (125 MHz, CD_3OD): δ 12.65, 28.00, 40.09, 50.71, 104.07, 111.91, 123.57, 126.41, 126.64, 129.92, 142.93, 143.23, 155.72, 174.50; HRMS-ESI (m/z): Exact mass calcd for $C_{29}H_{35}N_2$ $[M]^+$ 411.2795, found 411.2812.

Optical Characterization. Absorbance and emission profiles for each dye were obtained using both a Varian Cary 6000i UV−vis NIR Spectrophotometer using a data interval of 0.25 nm, a scan rate of 150 nm/min, a bandwidth of 2 nm, and a Varian Cary Eclipse Fluorescence Spectrophotometer, using a scan rate of 120 nm/min and a bandwidth of 5 nm. Anhydrous methanol was used as the spectroscopic solvent utilizing 1 cm cuvettes for both absorbance and emission readings. Molecular extinction coefficient values were determined by finding the slope of the concentration versus absorbance at λ_{max}. Quantum yields were determined in triplicate by comparing novel dyes **1**−**3** to reference dyes (Figure 2) with established quantum yields.[35] 3,3-Diethyloxacarbocyanine iodide was purchased from Sigma-Aldrich, astrophloxine was purchased from Toronto Research Chemicals, and 1-ethyl-2-((1*E*,3*E*)-5-((*E*)-1-ethyl-3,3-dimethylindolin-2-ylidene)penta-1,3-dien-1-yl)-3,3-dimethyl-3*H*-indol-1-ium 2,2,2-trifluoroacetate (**13**) was synthesized. Dilution series' were made with a maximum absorbance of 0.1 at the prescribed wavelength (based on the reference dye) to ensure minimization of the inner filter effect and nonradiative emission caused by aggregation. Emission spectra for the novel dyes **1**−**3** along with the CyDye DIGE fluors were collected using the same excitation wavelength and parameters used to find the quantum yield of the standard dyes. Absorbance max, emission max, quantum yields, and extinction coefficients are listed in Table 1.

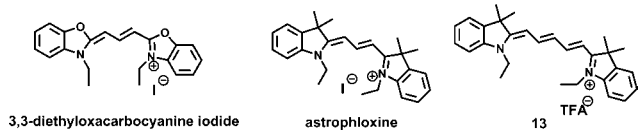

Figure 2. Structure of reference dyes 3,3-diethyloxacarbocyanine iodide, astrophloxine, and **13**.

Table 1. Optical Characterization of Z-CyDyes 1−3 and CyDye DIGE Fluors 4−6

dye	λ_{max} (nm)	Em_{max} (nm)	QY (%)	ε (M^{-1} cm^{-1})[a]
1 (Z-Cy2)	485	500	7[b]	155,000
2 (Z-Cy3)	548	564	11[c]	124,500
3 (Z-Cy5)	642	663	43[d]	216,200
4 (Cy2)	485	500	6[b]	150,300
5 (Cy3)	548	564	10[c]	137,600
6 (Cy5)	642	661	37[d]	214,400

[a]Molar extinction coefficients determined in methanol. [b]Quantum yield determined by exciting at 450 nm in methanol against 3,3-diethyloxacarbocyanine iodide.[35] [c]Quantum yield determined by exciting at 500 nm in methanol against astrophloxine.[35] [d]Quantum yield determined by exciting at 590 nm in methanol against **13**.[35]

2D Gel electrophoresis of CyDye DIGE Fluors vs Z-CyDyes. *Materials.* The protease inhibitor cocktail was purchased from Roche. The BCA Protein Assay Kit was purchased from Bio-Rad. DTT, ASB-14, and DMF were purchased from Sigma. All other reagents including buffers, IPG carrier ampholytes, precast IPG strips, and Cy2, Cy3, and Cy5 DIGE fluors were purchased from GE Healthcare or synthesized.[34] The urea lysis buffer consists of 30 mM Tris-HCl pH 8.5, 7 M urea, 2 M thiourea, 4% CHAPS, 1% ASB-14, 50 mM DTT, 0.5% IPG carrier ampholytes, and protease inhibitor cocktail. The urea labeling buffer consists of 30 mM Tris-HCl pH 8.5, 7 M urea, 2 M thiourea, 4% CHAPS, and 1% ASB-14. The urea rehydration buffer consists of 7 M urea, 2 M thiourea, 4% CHAPS, 1% ASB-14, 50 mM DTT, and 0.5% IPG carrier ampholytes.

Culturing of S. solfataricus. Liquid cultures of *S. solfataricus* (P2) were grown aerobically as previously described[36] in DSMZ media 182 (22.78 mM KH_2PO_4, 18.90 mM $(NH_4)_2SO_4$, 0.81 mM $MgSO_4$, 1.7 mM $CaCl_2$, 0.2% Yeast Extract) pH adjusted to 2.8 with 6N H_2SO_4. All cultures were grown in long neck Erlenmeyer flasks at 80 °C until OD_{650} = 0.3.

Protein Preparation. S. solfataricus (P2) cells were harvested by centrifugation at 5000*g* at 4 °C for 15 min and washed with ice-cold PBS. Pelleted cells were broken by freeze and thaw followed by solubilization in urea lysis buffer. After the supernatant was clarified by centrifugation, soluble proteins were purified and concentrated by precipitation with 5-fold volume ice-cold acetone, and solubilized for 1 h in urea lysis buffer. Protein concentration was measured with the BCA Protein Assay Kit. Samples were kept at −80 °C prior to labeling.

2D-DIGE Experimental Design and Analysis. S. solfataricus (P2) protein samples were subsequently labeled with CyDyes or Z-CyDyes according to the standard protocol from GE Healthcare. Briefly, 50 μg of each protein extract was labeled separately on ice in the dark for 30 min with 400 pmol of the *N*-hydroxysuccinimide esters of CyDye DIGE fluors (Cy2, Cy3,

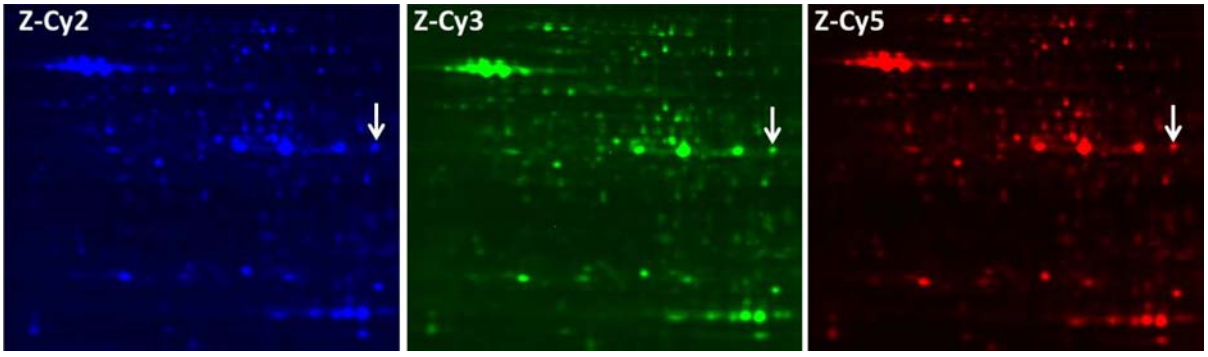

Figure 3. 2D gel of total soluble protein from *Sulfolobus solfataricus* labeled with Z-CyDyes. Each dye was used to label the protein sample separately. Dye labeled protein samples were combined and run on the same gel. After separation, the gel was scanned with 100 μm steps using the following laser excitation/band-pass filter combinations: 488/520 nm for Z-Cy2 (left), 532/580 nm for Z-Cy3 (middle), and 633/670 nm for Z-Cy5 (right). The white arrow indicates spot #197 (see Figure 6 for 3D visualization of spot #197). Images show the relatively crowded central region of the gel (pI 4−9 and 15−150 kDa), revealing well-defined spots with all three dyes.

and Cy5) or the novel Z-CyDyes (Z-Cy2, Z-Cy3, and Z-Cy5) dissolved in 99.8% DMF. Labeling reactions were performed in urea labeling buffer and were quenched by the addition of 2 μL of a 10 mM L-lysine solution and left on ice for 10 min. Appropriate labeled samples with Cy2, Z-Cy2, Cy3, Z-Cy3, Cy5, and Z-Cy5 were combined and mixed with up to 450 μL of urea rehydration buffer. 2-DE was performed as described elsewhere,[36,37] using precast IPG strips (pH 3−11 carrier ampholytes and protease inhibitor cocktail, nonlinear, 24 cm length) in the first dimension (IEF). Typically, 150 μg proteins were loaded on each IPG strip and IEF was carried out with the IPGPhor II isoelectric focusing system (GE Healthcare). Focusing was carried out at 20 °C, with a maximum of 50 μA/strip. Active rehydration was achieved by applying 50 V for 12 h. This was followed by a stepwise progression of 500 V gradient ramp to 8000 V for a total of 44 000 Vh. After IEF separation, the strips were equilibrated twice for 15 min with 50 mM Tris-HCl, pH 8.8, 6 M urea, 30% glycerol, 2% SDS, and a trace of bromophenol blue. The first equilibration solution contained 65 mM DTT, and 53 mM iodoacetamide was added in the second equilibration step instead of DTT. Second-dimension SDS-PAGE was performed in Dalt II (GE Healthcare) using 1-mm-thick, 24-cm, 12% polyacrylamide gels, and electrophoresis was carried out at a constant current (1 W/gel for 1 h, then at 2 W/gel for ∼16 h at 21 °C). Electrophoresis was completed once the bromophenol blue dye front reached the bottom of the gel. Two separate gels were labeled using either the 3 CyDyes purchased from GE Healthcare or the 3 Z-CyDyes. The gel image using Z-CyDyes is seen in Figure 3. The comparison of the number of spots vs dye is seen in Figure 4.

For DIGE experiments, previously synthesized Cy2, Cy3, and Cy5 were used according to the standard protocol from GE Healthcare. Two groups of identical normal soluble *S. solfataricus* protein fractions (3 technical replicates each) were labeled with either Z-Cy3, Z-Cy5, Cy3, or Cy5. The internal standard for the 6 gels were pooled together and labeled with Cy2 and run on each gel. Comparison of the spot volume vs dye is seen in Figure 5. Figure 6 shows the illustration of volumes for a single spot (spot #197) and a graph of spot volume vs spot number is seen in Figure 7.

Image Acquisition and Analysis. Gels were scanned using the Typhoon Trio Fluorescence Imager according to the manufacturer's protocol (GE Healthcare). Scans were acquired at 100 μm resolution at 600 V for PMT. Images were subjected to automated difference in gel analysis using Progenesis

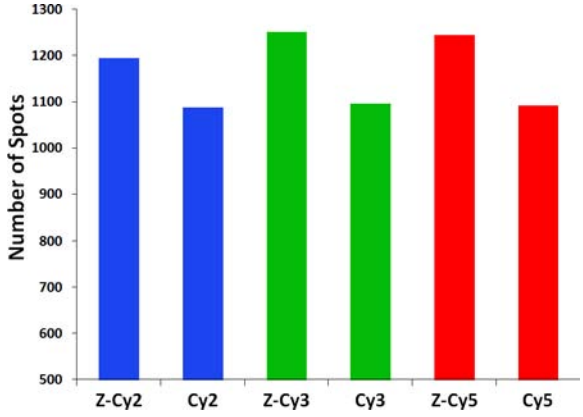

Figure 4. Total number of spots detected from a gel using Z-Cy2, Z-Cy3, and Z-Cy5 (see Figure 3 for images) and from a matched gel using Cy2, Cy3, and Cy5 purchased from GE Healthcare. The protein samples labeled and experimental protocols were the same for both gels and all dyes. Progenesis SameSpots software detects more spots when Z-CyDyes are used in comparison to CyDyes.

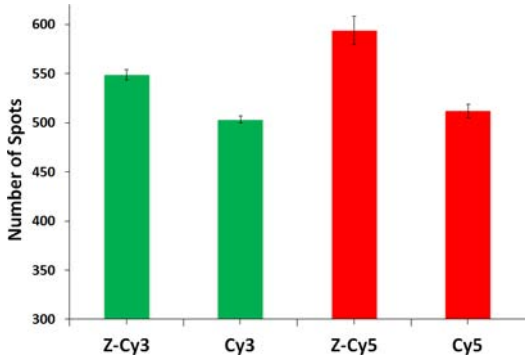

Figure 5. Standard 2D-DIGE comparison of protein spot numbers detected with Z-Cy3 and Cy3 (green) and Z-Cy5 and Cy5 (red). Triplicate analysis using DIGE protocol with a Cy2 internal reference detects a significant increase in spot number when Z-CyDyes are used in comparison to CyDyes (p = 0.0006). The lengths of the error bars represent the standard deviations.

SameSpots software version 3.1.v (Nonlinear Dynamics Ltd.). The Cy2 and Z-Cy2 gel images were scanned at an excitation wavelength of 488 nm with 520 nm emission wavelength filter, Cy3 and Z-Cy3 gel images were scanned at an excitation

dx.doi.org/10.1021/bc4002213 | *Bioconjugate Chem.* 2013, 24, 1552−1561

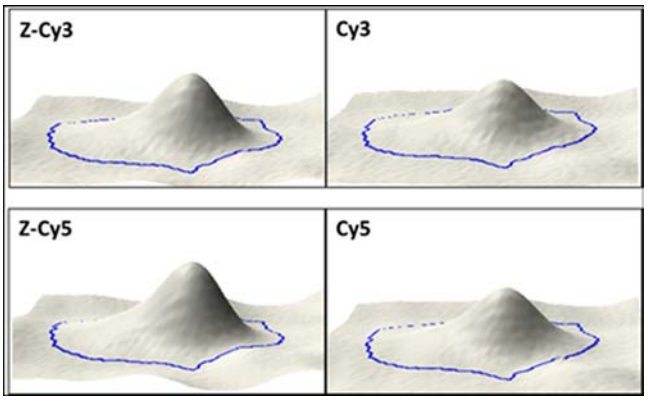

Figure 6. Illustration of volumes for a single spot (spot #197) labeled with the four dyes, as analyzed with Progenesis SameSpots software.

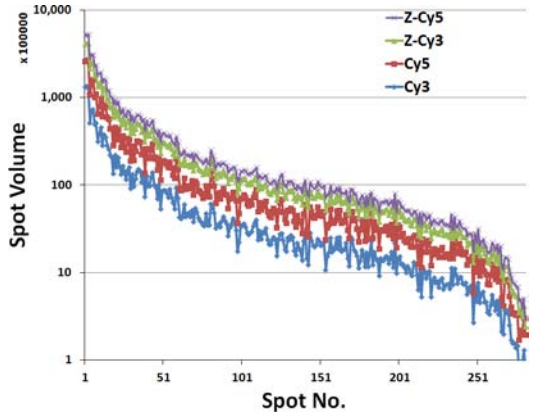

Figure 7. Average spot volumes (from triplicate 2D-DIGE analyses) vs spot number, when labeled with Z-Cy5 (purple), Z-Cy3 (green), Cy5 (red), and Cy3 (blue). Spot volumes follow a general trend of Z-Cy5 > Z-Cy3 > Cy5 > Cy3.

wavelength of 532 nm with an emission wavelength filter of 580 nm, while Cy5 and Z-Cy5 gel images were scanned at an excitation wavelength of 633 with an emission wavelength filter of 670 nm. Gel spots were co-detected as DIGE image pairs, which were linked to the corresponding in-gel Cy2 standard. Between gel comparisons were performed utilizing the in-gel standard from each image pair, using Progenesis SameSpots software. Out of approximately 500 spots identified, the spot volumes for 281 spots were measured. These spots were chosen for their well-defined boundaries and ranged in intensity from strong spots to faint spots. The normalized volume used in the comparison is a logarithmic ratio of a given dye over the internal standard dye, Cy2. Appendix SI-A (see Supporting Information) lists the data from the Z-Cy3 vs Cy3 DIGE Fluor spot volume comparison and the data from the Z-Cy5 vs Cy5 DIGE Fluor spot volume comparison.

RESULTS AND DISCUSSION

The Z-CyDyes (**1**−**3**) were synthesized by coupling of Cy2 (**4**), Cy3 (**5**), and Cy5 (**6**), respectively, with the titratable, cysteic acid linker **9** (Scheme 1) followed by activation of the carboxyl group. CyDyes **4**−**6** were prepared using the procedures reported by Jung et al.[34]

The side chain linker **9**, which is common to all three Z-CyDyes, is synthesized from *N*-methylcaprolactam in nine steps (Scheme 1). Hydrolysis of *N*-methylcaprolactam followed by protection of the secondary amine as its trifluoroacetate derivative and conversion of the resulting carboxylic acid into a *t*-butyl ester provided **7**. Deprotection of the amine and sequential reaction with *N*-Boc-bromoethylamine followed by global deprotection with trifluoroacetic acid and triethylsilane afforded the primary amine which was coupled with Boc-Cys(Trt)-OSu providing **8**. Simultaneous deprotection of the trityl and Boc groups and subsequent oxidation of the resultant thiol provided **9**.

The coupling of the three fluorophores **4**−**6** with the side chain **9** was accomplished in DMF in the presence of *N*-methylmorpholine to provide compounds **10**−**12**. Subsequent activation of the resulting free carboxylic acids as succinimidyl esters provided Z-CyDyes **1**−**3** (Scheme 2).

The absorbance maxima, emission maxima, extinction coefficients, and quantum yields of Z-CyDyes **1**−**3** as well as Cy2, Cy3, and Cy5 were determined and the data is shown in Table 1. The absorbance and emission maxima are unperturbed by the addition of side chain **9** as expected and therefore the same optical gel imaging protocol can be used for either dye set. The quantum yields of Z-CyDyes show a slight increase in comparison to their CyDye counterparts, although the differences do not warrant a change in the gel imaging protocol.

To test the performance of Z-CyDyes on 2D gels, the total soluble protein from the thermophillic archaea *Sulfolobus solfataricus*[38] was labeled with each dye (400 pmol/50 μg protein). The three samples were combined and subjected to 3−11 isoelectric focusing on 24 cm strips. The second dimension SDS-PAGE analysis used 12% gels. Each gel was scanned three times, once for each dye color. Visualization of 2D gel images created with Z-CyDyes confirmed that the labeled proteins were well focused with respect to pI and molecular weight (Figure 3).

Scheme 1. Synthesis of Side Chain 9

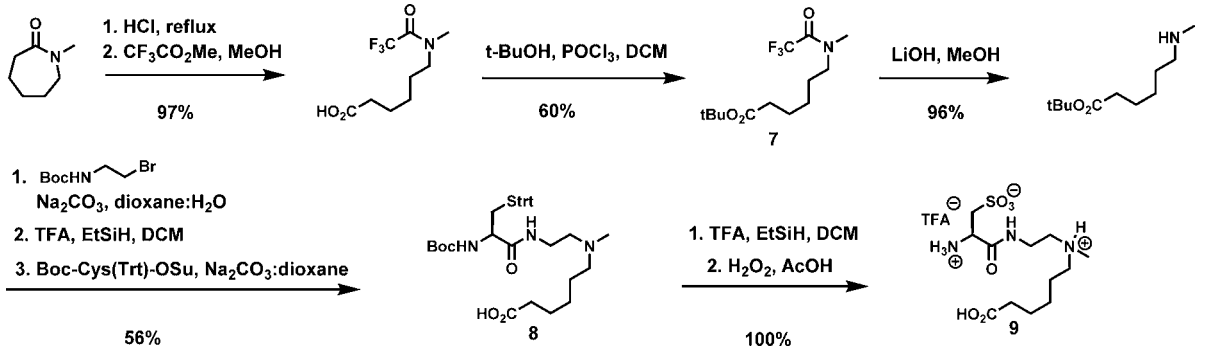

dx.doi.org/10.1021/bc4002213 | *Bioconjugate Chem.* 2013, 24, 1552−1561

Scheme 2. Reaction of 4, 5, and 6 with Side Chain 9 to Form 10, 11, and 12 and Subsequent Activation of the Carboxylic Acid to Form 1, 2, and 3

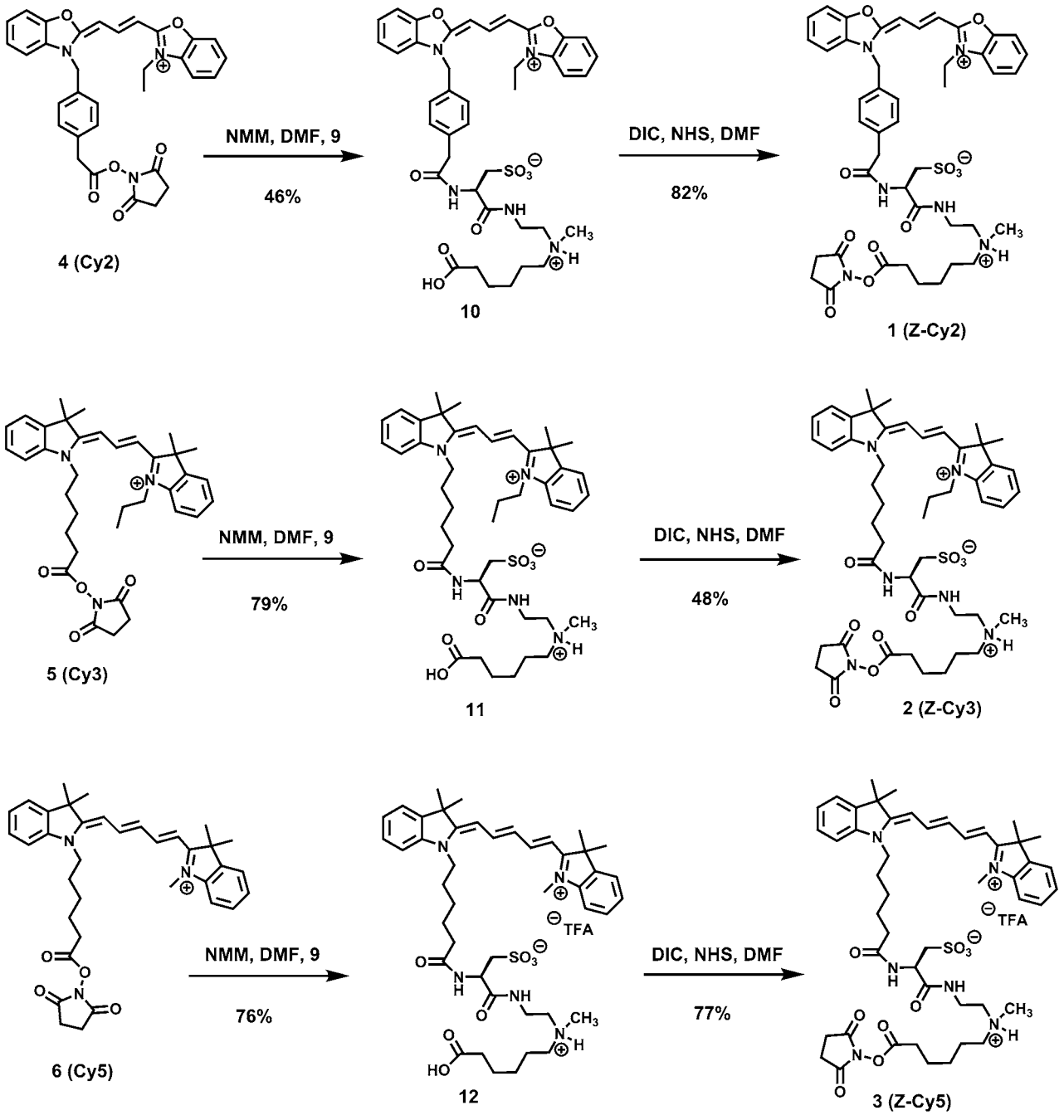

In parallel to the Z-CyDye experiment, the same protein sample was analyzed using standard Cy2, Cy3, and Cy5 purchased from GE Healthcare. Spot detection, using Progenesis SameSpots, showed an increase in the number of spots that were detected when employing Z-CyDyes in comparison to CyDyes (Figure 4).

Gel to gel variation resulting from sample loading, protein separation, and background was the driving force behind development of 2D-DIGE. While gel to gel variability still remains a challenge, the addition of a pooled internal standard[8] has facilitated quantitative analysis of differences in protein concentrations and PTMs across sets of gels. Cy2 is most commonly used as the internal standard in 2D-DIGE experiments. Therefore, to make a definitive analysis of Z-CyDyes, the experiments described above comparing Z-Cy3 vs Cy3 and Z-Cy5 vs Cy5 were repeated in triplicate, using Cy2 as the internal standard on all gels. Synthesized Cy2, Cy3, and Cy5 were used in order to address concerns that the increase in spot number in Figure 4 was from differences in purity between the commercial CyDyes and Z-CyDyes. A central region of the 2D gel was selected for comparison that was free of spot streaking and had low background. Progenesis SameSpots analysis revealed a significantly higher spot count from protein samples labeled with Z-CyDyes (Figure 5). Since Z-CyDyes have a higher spot count when compared with both commercial and synthesized CyDyes, this strongly suggested that structural differences and not sample purity were the cause.

dx.doi.org/10.1021/bc4002213 | *Bioconjugate Chem.* 2013, 24, 1552−1561

Visualization of 2D gels labeled with Z-CyDyes suggested that the spots were more intense in comparison to CyDyes. To quantify spot volume, Progenesis SameSpots software was employed as illustrated for spot #197 in Figure 6. Each spot used in the comparative analysis was manually inspected to ensure that the included volume (region inside the perimeter) was centered on each spot and was not overlapping other peaks.

Out of all spots available, 281 spots adhered to the standards shown in Figure 6 in all 6 gels, and were used to quantify spot volumes, as shown in Figure 7. Spot intensity was consistently greater for Z-CyDyes compared to CyDyes. The data shows that Z-Cy5 was more intense than Z-Cy3 and Cy5 was more intense than Cy3.

CONCLUSION

In summary, a new set of fluorescent dyes for protein amine labeling have been synthesized that show enhanced sensitivity relative to CyDyes. The optical properties of the Z-CyDye DIGE fluors reported herein are similar to the commercial CyDye DIGE fluors. In addition, the Z-CyDyes have been shown to be compatible with labeling, gel separation, and imaging protocols used in 2D-DIGE experiments. The increase in spot number and volume for Z-CyDyes is consistent with the hypothesis that the more water-soluble dyes decrease protein precipitation leading to an increase in dye labeled protein for 2D-DIGE analysis. The increased sensitivity will allow for a more thorough study of the proteome and aid in the identification of proteins and protein isoforms with low copy numbers.

ASSOCIATED CONTENT

Supporting Information

Appendix SI-A lists the data from the Z-Cy3 vs Cy3 DIGE Fluor and Z-Cy5 vs Cy5 DIGE Fluor spot volume comparison. This material is available free of charge via the Internet at http://pubs.acs.org.

AUTHOR INFORMATION

Corresponding Author

*E-mail: grieco@chemistry.montana.edu. Fax: +(406) 994-5407.

Notes

The authors declare no competing financial interest.

ACKNOWLEDGMENTS

We thank the National Institute of Health (CoBRE 5P20RR024237-04 and P20GM104935-05, EAD, PI) for funding this work. B.B. receives support from the National Science Foundation, MCB102248. The Mass Spectrometry, Proteomics and Metabolomics core facility receives support from the Murdock Charitable Trust and INBRE MT Grant No. P20 RR-16455-08.

REFERENCES

(1) Pandey, A., and Mann, M. (2000) Proteomics to study genes and genomes. *Nature 405* (6788), 837−846.

(2) Aebersold, R., and Mann, M. (2003) Mass spectrometry-based proteomics. *Nature 422* (6928), 198−207.

(3) Mann, M., and Jensen, O. N. (2003) Proteomic analysis of post-translational modifications. *Nat. Biotechnol. 21* (3), 255−261.

(4) Pawson, T., and Nash, P. (2003) Assembly of cell regulatory systems through protein interaction domains. *Science 300* (5618), 445−452.

(5) Tyson, J. J., Chen, K. C., and Novak, B. (2003) Sniffers, buzzers, toggles and blinkers: dynamics of regulatory and signaling pathways in the cell. *Curr. Opin. Cell Biol. 15* (2), 221−231.

(6) Unlu, M., Morgan, M. E., and Minden, J. S. (1997) Difference gel electrophoresis: A single gel method for detecting changes in protein extracts. *Electrophoresis 18* (11), 2071−2077.

(7) Tonge, R., Shaw, J., Middleton, B., Rowlinson, R., Rayner, S., Young, J., Pognan, F., Hawkins, E., Currie, I., and Davison, M. (2001) Validation and development of fluorescence two-dimensional differential gel electrophoresis proteomics technology. *Proteomics 1* (3), 377−396.

(8) Alban, A., David, S. O., Bjorkesten, L., Andersson, C., Sloge, E., Lewis, S., and Currie, I. (2003) A novel experimental design for comparative two-dimensional gel analysis: Two-dimensional difference gel electrophoresis incorporating a pooled internal standard. *Proteomics 3* (1), 36−44.

(9) Marouga, R., David, S., and Hawkins, E. (2005) The development of the DIGE system: 2D fluorescence difference gel analysis technology. *Anal. Bioanal. Chem. 382* (3), 669−678.

(10) Zhou, G., Li, H. M., DeCamp, D., Chen, S., Shu, H. J., Gong, Y., Flaig, M., Gillespie, J. W., Hu, N., Taylor, P. R., Emmert-Buck, M. R., Liotta, L. A., Petricoin, E. F., and Zhao, Y. M. (2002) 2D differential in-gel electrophoresis for the identification of esophageal scans cell cancer-specific protein markers. *Molecular & Cellular Proteomics 1* (2), 117−124.

(11) Gharbi, S., Gaffney, P., Yang, A., Zvelebil, M. J., Cramer, R., Waterfield, M. D., and Timms, J. F. (2002) Evaluation of two-dimensional differential gel electrophoresis for proteomic expression analysis of a model breast cancer cell system. *Molecular & Cellular Proteomics 1* (2), 91−98.

(12) Somiari, R. I., Sullivan, A., Russell, S., Somiari, S., Hu, H., Jordan, R., George, A., Katenhusen, R., Buchowiecka, A., Arciero, C., Brzeski, H., Hooke, J., and Shriver, C. (2003) High-throughput proteomic analysis of human infiltrating ductal carcinoma of the breast. *Proteomics 3* (10), 1863−1873.

(13) Friedman, D. B., Hill, S., Keller, J. W., Merchant, N. B., Levy, S. E., Coffey, R. J., and Caprioli, R. M. (2004) Proteome analysis of human colon cancer by two-dimensional difference gel electrophoresis and mass spectrometry. *Proteomics 4* (3), 793−811.

(14) Lee, I. N., Chen, C. H., Sheu, J. C., Lee, H. S., Huang, G. T., Yu, C. Y., Lu, F. J., and Chow, L. P. (2005) Identification of human hepatocellular carcinoma-related biomarkers by two-dimensional difference gel electrophoresis and mass spectrometry. *J. Proteome Res. 4* (6), 2062−2069.

(15) Perrin, R. J., Craig-Schapiro, R., Malone, J. P., Shah, A. R., Gilmore, P., Davis, A. E., Roe, C. M., Peskind, E. R., Li, G., Galasko, D. R., Clark, C. M., Quinn, J. F., Kaye, J. A., Morris, J. C., Holtzman, D. M., Townsend, R. R., and Fagan, A. M. (2011) Identification and validation of novel cerebrospinal fluid biomarkers for staging early Alzheimer's disease. *Plos One 6* (1), e16032.

(16) Chou, J. L., Shenoy, D. V., Thomas, N., Choudhary, P. K., LaFerla, F. M., Goodman, S. R., and Breen, G. A. M. (2011) Early dysregulation of the mitochondrial proteome in a mouse model of Alzheimer's disease. *J. Proteomics 74* (4), 466−479.

(17) Takano, M., Yamashita, T., Nagano, K., Otani, M., Maekura, K., Kamada, H., Tsunoda, S.-I., Tsutsumi, Y., Tomiyama, T., Mori, H., Matsuura, K., and Matsuyama, S. (2013) Proteomic analysis of the hippocampus in Alzheimer's disease model mice by using two-dimensional fluorescence difference in gel electrophoresis. *Neurosci. Lett. 534*, 85−9.

(18) Nagalla, S. R., Canick, J. A., Jacob, T., Schneider, K. A., Reddy, A. P., Thomas, A., Dasari, S., Lu, X., Lapidus, J. A., Lambert-Messerlian, G. M., Gravett, M. G., Roberts, C. T., Jr., Luthy, D., Malone, F. D., and D'Alton, M. E. (2007) Proteomic analysis of maternal serum in Down syndrome: Identification of novel protein biomarkers. *J. Proteome Res. 6* (4), 1245−1257.

(19) Shaw, J., Rowlinson, R., Nickson, J., Stone, T., Sweet, A., Williams, K., and Tonge, R. (2003) Evaluation of saturation labelling two-dimensional difference gel electrophoresis fluorescent dyes. *Proteomics 3* (7), 1181−1195.
(20) Kondo, T., and Hirohashi, S. (2006) Application of highly sensitive fluorescent dyes (CyDye DIGE Fluor saturation dyes) to laser microdissection and two-dimensional difference gel electrophoresis (2D-DIGE) for cancer proteomics. *Nat. Protoc. 1* (6), 2940−2956.
(21) Leonard, S. E., and Carroll, K. S. (2013) Chemical 'omics' approaches for understanding protein cysteine oxidation in biology. *Curr. Opin. Chem. Biol. 15* (1), 88−102.
(22) Eaton, P. (2006) Protein thiol oxidation in health and disease: Techniques for measuring disulfides and related modifications in complex protein mixtures. *Free Radical Biol. Med. 40* (11), 1889−1899.
(23) Ying, J., Clavreul, N., Sethuraman, M., Adachi, T., and Cohen, R. A. (2007) Thiol oxidation in signaling and response to stress: Detection and quantification of physiological and pathophysiological thiol modifications. *Free Radical Biol. Med. 43* (8), 1099−1108.
(24) Ernst, L. A., Gupta, R. K., Mujumdar, R. B., and Waggoner, A. S. (1989) Cyanine dye labeling reagents for sulfhydryl-groups. *Cytometry 10* (1), 3−10.
(25) Mujumdar, S. R., Mujumdar, R. B., Grant, C. M., and Waggoner, A. S. (1996) Cyanine-labeling reagents: Sulfobenzindocyanine succinimidyl esters. *Bioconjugate Chem. 7* (3), 356−362.
(26) Mujumdar, R. B., Ernst, L. A., Mujumdar, S. R., Lewis, C. J., and Waggoner, A. S. (1993) Cyanine dye labeling reagents - sulfoindocyanine succinimidyl esters. *Bioconjugate Chem. 4* (2), 105−111.
(27) Buschmann, V., Weston, K. D., and Sauer, M. (2003) Spectroscopic study and evaluation of red-absorbing fluorescent dyes. *Bioconjugate Chem. 14* (1), 195−204.
(28) Gruber, H. J., Hahn, C. D., Kada, G., Riener, C. K., Harms, G. S., Ahrer, W., Dax, T. G., and Knaus, H. G. (2000) Anomalous fluorescence enhancement of Cy3 and Cy3.5 versus anomalous fluorescence loss of Cy5 and Cy7 upon covalent linking to IgG and noncovalent binding to avidin. *Bioconjugate Chem. 11* (5), 696−704.
(29) Mader, O., Reiner, K., Egelhaaf, H. J., Fischer, R., and Brock, R. (2004) Structure property analysis of pentamethine indocyanine dyes: Identification of a new dye for life science applications. *Bioconjugate Chem. 15* (1), 70−78.
(30) Pham, W., Medarova, Z., and Moore, A. (2005) Synthesis and application of a water-soluble near-infrared dye for cancer detection using optical imaging. *Bioconjugate Chem. 16* (3), 735−740.
(31) Bouteiller, C., Clave, G., Bernardin, A., Chipon, B., Massonneau, M., Renard, P.-Y., and Romieu, A. (2007) Novel water-soluble near-infrared cyanine dyes: Synthesis, spectral properties, and use in the preparation of internally quenched fluorescent probes. *Bioconjugate Chem. 18* (4), 1303−1317.
(32) Markova, L. I., Fedyunyayeva, I. A., Povrozin, Y. A., Semenova, O. M., Khabuseva, S. U., Terpetschnig, E. A., and Patsenker, L. D. (2013) Water soluble indodicarbocyanine dyes based on 2,3-dimethyl-3-(4-sulfobutyl)-3H-indole-5-sulfonic acid. *Dyes Pigm. 96* (2), 535−546.
(33) Wang, L., Fan, J., Qiao, X., Peng, X., Dai, B., Wang, B., Sun, S., Zhang, L., and Zhang, Y. (2010) Novel asymmetric Cy5 dyes: Synthesis, photostabilities and high sensitivity in protein fluorescence labeling. *J. Photochem. Photobiol., A 210*, 168−172.
(34) Jung, M. E., and Kim, W. J. (2006) Practical syntheses of dyes for difference gel electrophoresis. *Bioorg. Med. Chem. 14* (1), 92−97.
(35) Waggoner, A., Debiasio, R., Conrad, P., Bright, G. R., Ernst, L., Ryan, K., Nederlof, M., and Taylor, D. (1989) Multiple spectral parameter imaging. *Methods Cell Biol. 30*, 449−478.
(36) Maaty, W. S., Wiedenheft, B., Tarlykov, P., Schaff, N., Heinemann, J., Robison-Cox, J., Valenzuela, J., Dougherty, A., Blum, P., Lawrence, C. M., Douglas, T., Young, M. J., and Bothner, B. (2009) Something old, something new, something borrowed; how the thermoacidophilic archaeon sulfolobus solfataricus responds to oxidative stress. *Plos One 4* (9), e6964.
(37) Barry, R. C., Young, M. J., Stedman, K. M., and Dratz, E. A. (2006) Proteomic mapping of the hyperthermophilic and acidophilic archaeon Sulfolobus solfataricus P2. *Electrophoresis 27* (14), 2970−2983.
(38) Zillig, W., Stetter, K. O., Wunderl, S., Schulz, W., Priess, H., and Scholz, I. (1980) The sulfolobus-caldariella group - taxonomy on the basis of the structure of DNA-dependent RNA-polymerases. *Arch. Microbiol. 125* (3), 259−269.